Supporting Information

In situ alloying of thermally conductive polymer composites by combining liquid and solid metal micro-additives

Matthew I. Ralphs,[1] Nicholas Kemme,[1] Prathamesh B. Vartak,[1] Emil Joseph,[1] Sujal Tipnis,[1] Scott Turnage,[1] Kiran N. Solanki,[1], Robert Y. Wang,[1,] and Konrad Rykaczewski[1,*]*

*email: konradr@asu.edu and rywang@asu.edu

SBA AND ASTM D5470 STANDARD BASICS

The sample temperature drop is determined by extrapolating the linear temperature distribution from the bottom bar to the bottom of the sample and a 2nd order curve fit from the end of the top bar to the top of the sample, as outlined by Thompson.[1] This method of using a 2nd order fit for the end of the top bar was used primarily to be consistent with the method laid out by Thompson, but the difference in using a 2nd order fit vs a 1st order fit is generally small (< 2%) for our samples. The heat flux through the reference bars is determined from the slope of its temperature distribution (i.e., Fourier's Law), as described by a linear fit through the measured temperatures in the bars. Only the upper portion of the top bar is used in the fit to calculate the heat flux in order to avoid any effects from the interface with the sample – though no effects have been specifically identified. **Figure S1a** demonstrates these principles as it applies to the stepped bar apparatus. **Figure S1b** presents measured values for small LM inclusions in PDMS at various values of ϕ, following the procedure as outlined by Jeong et al.[2] along with reported results by Jeong et al. The slight difference in values can be traced back to the k of the polymer matrix. They measure $k_{PDMS} = 0.17$ $Wm^{-1}K^{-1}$ and we measure $k_{PDMS} = 0.27$ $Wm^{-1}K^{-1}$, which difference follows through the rest of the values in the data. The difference in measured values of the PDMS could be due to difference in polymer or measurement technique. They used Elastosil RT 601 and we used Sylgard 184. They used xenon flash to measure thermal diffusivity and converted that to a thermal conductivity whereas we measured thermal resistance and sample thickness with an SBA to get thermal conductivity.

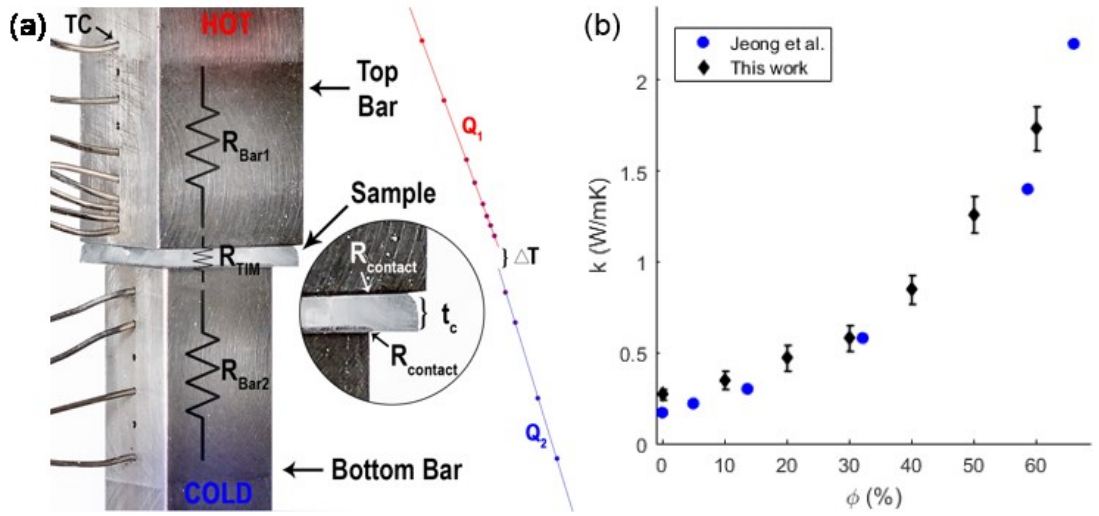

Figure S1: (a) Measurement principles of the ASTM D5470 standard. **(b)** Our results with well dispersed LM inclusions validated against Jeong et al.[2]

The thermal conductivity of the two stainless steel reference bars used in this work is approximately 14.5 W/m-K, but can vary from 14.1 $Wm^{-1}K^{-1}$ at 22°C to 14.7 $Wm^{-1}K^{-1}$ at 47°C, depending on the precise temperature of the upper or lower bar. An individual value is used for $k_{SS,top}$ and $k_{SS,bottom}$ and is updated with every measurement using the real time average temperature of each bar and is then fit to the thermal conductivity data of stainless steel from Assael and Gialou.[3]

PARTICLE SIZE DISTRIBUTIONS AND PROBABILITY DISTRIBUTIONS

The actual particle distributions in the well-dispersed composites are presented by the histograms in **Figure S2** with the respective probability distribution fits overlaid. The distributions were assumed to be normal even though some skewness is observed in the figure. These particle distributions were obtained by manual particle selection in ImageJ because the automatic

thresholding was not adequate to differentiate between individual particles and particles in close proximity to each other.

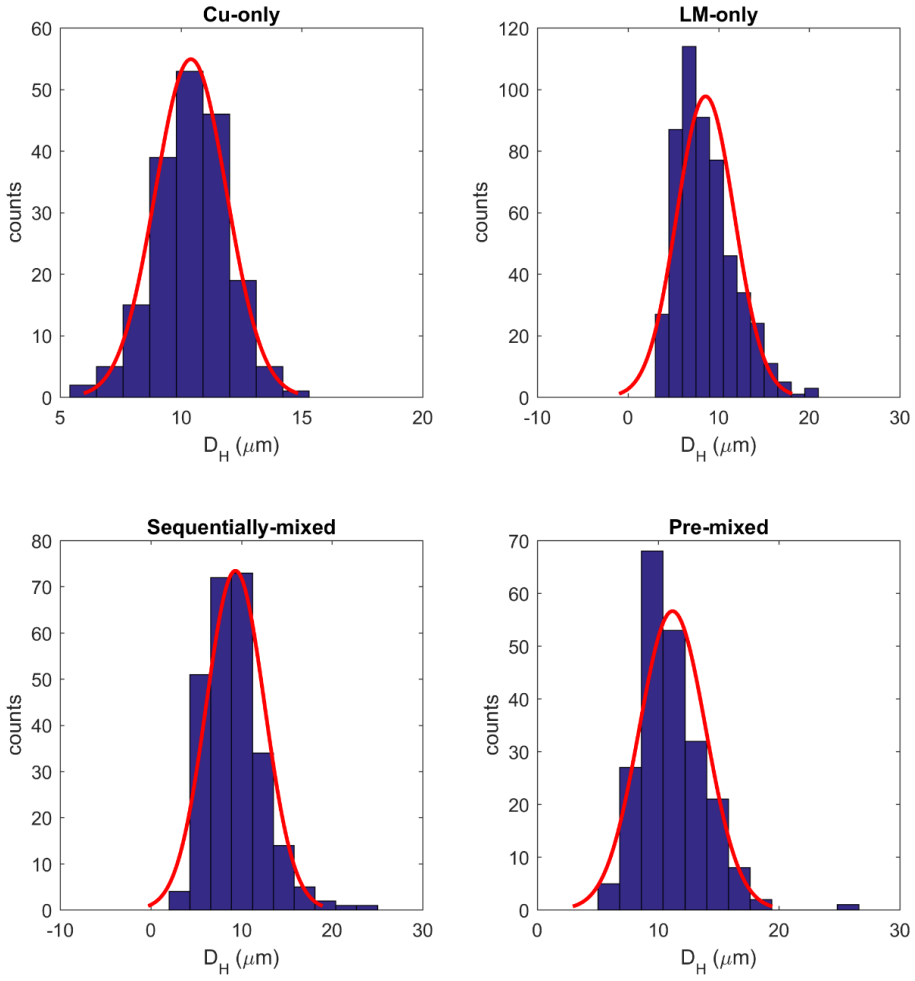

Figure S2: Particle distributions for the well dispersed samples with overlaying probability distribution fit.

TAVANGAR MODEL PARAMETERS

The parameters used for the Tavangar model in **Figure 3c** are as follows: $k_{p\ (LM)} = 26.2\ Wm^{-1}K^{-1}$, $k_{p\ (Cu)} = 400\ Wm^{-1}K^{-1}$, $R_b = 1\times10^{-7}\ m^2KW^{-1}$, $a = 5\times10^{-5}$ m, $L_{Cu} = 0.3333$, and $L_{LM} = 0.368$.

ESTIMATED THERMAL CONDUCTIVITY AFTER ACCOUNTING FOR CONTACT RESISTANCE BETWEEN THE REFERENCE BARS AND SAMPLES

Figure S3 shows the effective intrinsic thermal conductivity of the samples in this work after taking into account sample contact resistance. Large uncertainty bands on higher k values are due to the contact resistance composing a significant amount of the total measured resistance, R_{th}, and the somewhat large uncertainty of the value for R_c.

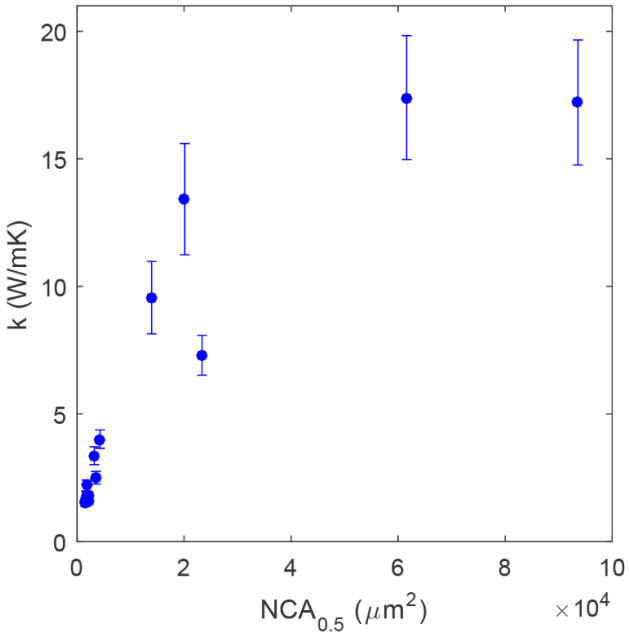

Figure S3: Estimated effective intrinsic thermal conductivity, $\bar{k}$, versus the 50th percentile NCA values. These thermal conductivity values are based upon the intrinsic thermal resistance of the sample as determined by subtracting out the contact resistance between the sample and reference bars from the total measured thermal resistance. Large uncertainties at higher thermal conductivities are a result of (i) our estimated values of R_c and (ii) R_c comprising an increasing proportion of the total measured thermal resistance at high thermal conductivities.

COMPOSITE CURED ON AL, LM BLEED ISSUE, SEM OF CU, AND TABULATED DATA USED IN FIGURE 3C AND S3.

Figure S4 is an image of the composite after curing in place between Al foil for 2 hours at 100°C with no visible signs of corrosion on the Al. **Figure S5** shows that the problem of LM bleeding out of a 50% LM composite is solved by adding in Cu to the composite: 25% LM, 25% Cu. **Figure S6** is an SEM of representative copper particles to those used in the composite. And **Table S1** is the tabulated data used in **Figure 3c** and **S3**.

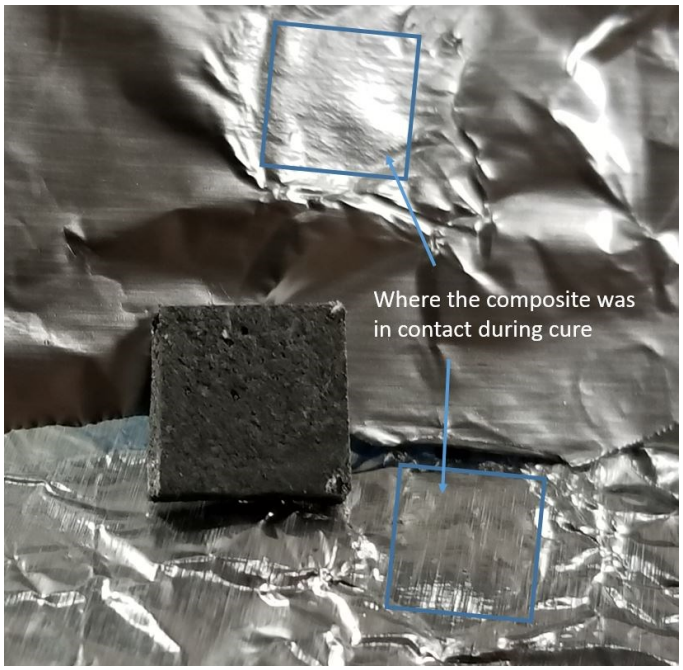

Figure S4: Composite with large LM-Cu colloids that was cured between aluminum foil with no corrosion apparent to the Al.

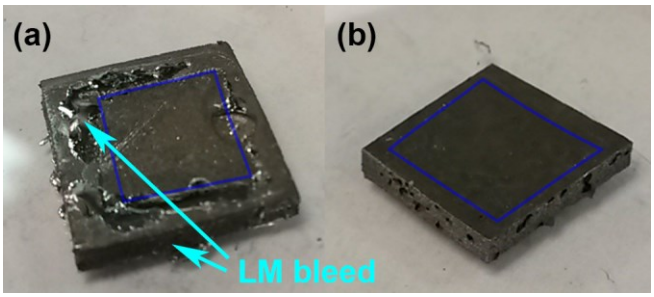

Figure S5: (a) 50% LM composite after 1.5 MPa square load applied and released, showing LM bleed and (b) 25% LM, 25% Cu composite after 3 MPa square load applied and released, showing no LM bleed at double the pressure. The blue squares designate where the load was applied.

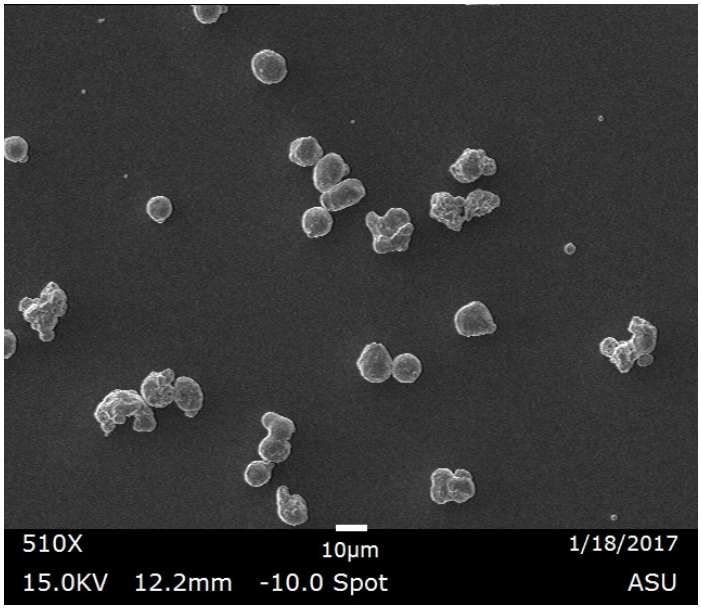

Figure S6: SEM of Copper particles used in the composites from Alfa Aesar, 10μm APS.

Table S1: Data used in Figure 3c and S3 which plot k_{eff} and k, respectively, for the samples with large LM-Cu colloids.

Sample #	k_{eff} (W/mK)	$U_{k_{eff}}$(68% CI)	K (W/mK)	U_k(68% CI)	$PAD_{50\%}$ (μm^2)
93	5.52	0.33	7.30	0.78	23367
92	3.40	0.20	4.01	0.36	4297
90	6.17	0.37	13.42	2.18	20130
89	5.09	0.31	9.56	1.42	13946
85	9.73	0.58	17.21	2.45	93603
75	1.50	0.09	1.62	0.12	1654
73	1.62	0.10	1.80	0.14	2083
71	1.60	0.10	1.80	0.15	1714
68	1.56	0.12	1.75	0.18	1938
59	2.10	0.15	2.50	0.25	3532
57	2.00	0.14	2.20	0.21	1759
55	1.50	0.12	1.52	0.15	1590
53	1.55	0.12	1.61	0.16	2110
50	1.45	0.10	1.55	0.15	1553
36	10.08	0.60	17.40	2.43	61589
33	2.78	0.20	3.36	0.35	3224

THERMAL GREASE PUMP-OUT

Most thermal greases undergo what is commonly known as pump-out, where the grease gets pumped out from between components due to thermal stresses in the system. Repeated thermal cycling from normal IC operation causes the grease to get squeezed between components and out of its desired location. Over time, this leaves air gaps between components, causing a thermal resistance similar to that with no thermal grease. Figure S7 demonstrates this issue with a commercial LM-based grease on only the first cycle, simulated by a 50g (5.4 kPa) load. Most thermal greases are designed to resist pump-out and postpone its negative effects. The grease in Figure S7 has extremely good thermal performance, but is more susceptible to pump-out than many other thermal greases because of its low viscosity.

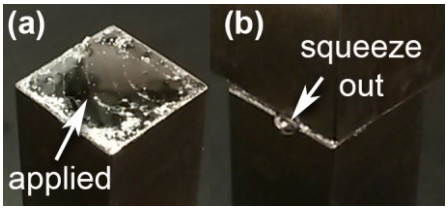

Figure S7: (a) Even application of LM-based commercial grease before applied pressure, (b) LM squeezed out of desired location under 50g (5.4 kPa) load.

MECHANICAL CHARACTERIZATION

The compressive modulus of the samples was measured using compression relaxation tests as seen in **Figure S8** performed on an Instron 5969 mechanical tester. Here samples are loaded through their thickness at a strain rate of 10^{-4} s^{-1} after a load of ~4 N. When the engineering stress in the sample reached 10 MPa, the load was reversed and the slope of the initial unloading was

measured as the material stiffness for the purpose of qualitative comparison. In order to determine whether the modulus measurement varied as a function of strain within the sample, the load was again reversed and the sample loaded to 20 MPa before a second relaxation. In the case of pure PDMS, the modulus was too low for the material to reach 10 MPa of stress without effects of inertia, so the first and second relaxations were performed when the sample compressed to approximately 25% and 50% strain, respectively. Modulus results (see Table S2), which can only be used to qualitatively compare the materials, indicate that the size of the LM-Cu colloids do not significantly affect the mechanical properties of the composite. Furthermore, our samples with large LM-Cu colloids have a modulus in the same range as a well dispersed PDMS composite with 50% copper particles ($10\mu m$ APS). The compressive modulus measured for pure PDMS (Sylgard 184) is similar to that measured by Johnston et al.[4]

Table S2: Estimated compressive modulus for various samples.

Material	First Modulus Result [MPa]	Second Modulus Result [MPa]
Pure PDMS	42	246
Sample #93 (k_{eff} = 5.5 $Wm^{-1}K^{-1}$)	748	936
Sample #36 (k_{eff} = 10.1 $Wm^{-1}K^{-1}$)	814	1082
PDMS 50% Cu	855	1552

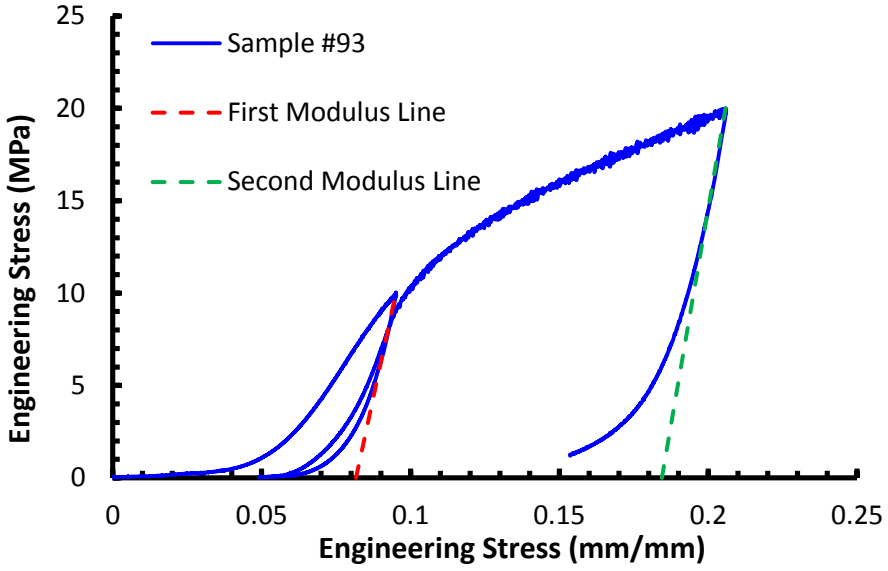

Figure S8: Stress-strain data showing how the compressive modulus values were obtained.

REFERENCES

(1) Thompson, D. R.; Rao, S. R.; Cola, B. A. A Stepped-Bar Apparatus for Thermal Resistance Measurements. *J. Electron. Packag.* **2013**, *135* (4), 41002.

(2) Jeong, S. H.; Chen, S.; Huo, J.; Gamstedt, E. K.; Liu, J.; Zhang, S.-L.; Zhang, Z.-B.; Hjort, K.; Wu, Z. Mechanically Stretchable and Electrically Insulating Thermal Elastomer Composite by Liquid Alloy Droplet Embedment. *Sci. Rep.* **2015**, *5* (November), 18257.

(3) Assael, M. J.; Gialou, K. Measurement of the Thermal Conductivity of Stainless Steel AISI 304L up to 550 K. *Int. J. Thermophys.* **2003**, *24* (4), 1145–1153.

(4) Johnston, I. D.; McCluskey, D. K.; Tan, C. K. L.; Tracey, M. C. Mechanical Characterization of Bulk Sylgard 184 for Microfluidics and Microengineering. *J. Micromechanics Microengineering* **2014**, *24*, 35017.